NASA Technical Memorandum 4125

A Three-Node C° Element for Analysis of Laminated Composite Sandwich Shells

C. Wayne Martin, S. F. Lung,
and K. K. Gupta
Ames Research Center
Dryden Flight Research Facility
Edwards, California

National Aeronautics and
Space Administration
Office of Management
Scientific and Technical
Information Division

1989

SUMMARY

A three-node flat shell element with C° rotation fields has been developed for analysis of arbitrary composite shells. The element may consist of any number of orthotropic layers, each layer having different material properties and angular orientation. The formulation includes coupling between bending and extension, which is essential for analysis of unsymmetric laminates. Shearing deflections are included, since laminated and sandwich construction frequently results in shear stiffness much smaller than bending stiffness. Formulation of the element is straightforward, and calculation of its stiffness matrix is simple and fast. Convergence of solutions with mesh refinement is uniform for both thin and thick shells and is insensitive to element shape, although not as rapid as some other elements that lack one or more capabilities of the newly developed element. An experimental verification of the shell element is reported in the appendix.

INTRODUCTION

Significant improvements in aircraft flutter speeds and other performance characteristics are possible through creative use of composite materials, as has been pointed out by Weisshaar (1987). Finite-element analysis of structures of this type requires shell elements representing layered composites that may be unsymmetric and may frequently use honeycomb or foam cores. The element described here was developed for this purpose.

Since the beginning of research on the finite-element method, a great deal of effort has been expended on development of shell elements. Many papers on this subject have been published (Gallagher, 1975; 1978). However, the perfect shell element has yet to be invented.

Triangular flat-elements having displacements and rotations at the corner nodes as degrees of freedom (dof) are appealing for practical reasons. They can easily model arbitrary shell geometries with general supports, cutouts, and beam stiffeners. These elements have a total of 18 dof (three translations and three rotations at each node) or 15 dof (three translations and two rotations), depending on whether the rotation about the normal, which has zero stiffness, is included as a degree-of-freedom.

One of the earliest shell elements was a flat triangular element developed by Melosh (1966) and Martin (1967). Versions of this element were used in several early programs including ELAS, SAMIS, and DYNAL. At that time, it was the only element that used the transverse shear modulus, and, consequently, it was the only element suitable for sandwich plates and shells. In 1971, Utku (1973) developed a new version with a straightforward treatment of shearing stiffness which is theoretically much improved.

The element developed here follows the derivation by Utku (1973). However, integration through the thickness is done stepwise, required for representing laminates, and two additional terms of the energy integrals are retained, since they do not vanish for unsymmetric laminates.

This element converges at about the same rate for thick or thin plates, regardless of element shape. It appears to be quite robust and is capable of correctly modeling behavior of general, unsymmetric, sandwich, laminated composite shells. Convergence is slower than that of some other three-node elements that do not include shearing deflections. Because of its straightforward formulation, this element may provide a basis for development of a dynamic element (Gupta, 1979), which could result in a significant improvement of numerical efficiency in analysis of problems of aircraft vibration and flutter.

ELEMENT FORMULATION

The triangular element is developed in a local coordinate system with origin at the middle surface centroid, and the x axis is parallel to the element 1–2 edge, as shown in figure 1. The z axis is perpendicular to the plane of the

element. In the computer implementation of the element, material properties for a layer are defined with respect to a material coordinate axis which may be oriented at an angle α measured from the element x axis to the material 1 axis. The material 3 axis coincides with the element z axis. Displacements in the x, y, z directions are denoted by u, v, w. The usual right-hand vector convention is used for directions of rotations, which are denoted by θ_x, θ_y, and θ_z. The rotations θ_x and θ_y are rotations of lines originally perpendicular to the middle surface of the undeformed element.

Using the comma convention for differentiation, the midsurface strains ϵ_o are given by

$$\epsilon_o = \begin{bmatrix} u_{o,x} \\ v_{o,y} \\ u_{o,y} + v_{o,x} \end{bmatrix}$$

and curvatures are given by

$$X = \begin{bmatrix} -\theta_{y,x} \\ \theta_{x,y} \\ \theta_{x,x} - \theta_{y,y} \end{bmatrix} = \begin{bmatrix} w'_{,xx} \\ w'_{,yy} \\ 2\,w'_{,xy} \end{bmatrix}$$

In this derivation, the total deflection w is in the z direction

$$w = w' + w^\star$$

where w' is the Kirchhoffian part of the deflection and $w^\star$ is the part due to out-of-plane shear.

At any point in the element, the strains are given by

$$\epsilon = \epsilon_o - zX$$

and stresses are given by

$$\sigma = D\epsilon = D\epsilon_o - DzX$$

where D is a 3 by 3 material property matrix for plane stress in the lamina.

The out-of-plane shear strains are given by

$$\gamma = \begin{bmatrix} \gamma_{xz} \\ \gamma_{yz} \end{bmatrix} = \begin{matrix} w^\star_{,x} \\ w^\star_{,y} \end{matrix}$$

and the corresponding shear stresses are given by

$$\tau = \begin{bmatrix} \tau_{xz} \\ \tau_{yz} \end{bmatrix} = D'\gamma = D' \begin{bmatrix} \gamma_{xz} \\ \gamma_{yz} \end{bmatrix}$$

The shear moduli in D' are reduced by a factor of 5/6 to account for nonuniform distribution of shear stress, as is done in many other programs.

In this formulation, a straight line, which is normal to the middle surface before loading, remains straight, but not normal to the deformed middle surface after loading. The slopes of the middle surface are $w_{,x}$ and $w_{,y}$, whereas the slopes of the line that was originally normal to the middle surface become $-\theta_y = w_{,x} - w^\star_{,x}$ and $\theta_x = w_{,y} - w^\star_{,y}$ and $\theta_x = -v_{,z}$ and $\theta_y = u_{,z}$.

The total strain energy in the element is given by

$$U = \frac{1}{2}\int \epsilon^T \sigma dA dz + \frac{1}{2}\int \gamma^T \tau dA dz$$

The energy expression can be expanded into five terms, as follows:

$$U = \frac{1}{2}\int \epsilon_o^T D \epsilon_o dA dz + \frac{1}{2}\int X^T D X z^2 dA dz + \frac{1}{2}\int \gamma^T D' \gamma dA dz + \frac{1}{2}\int X^T D \epsilon_o z dA dz + \frac{1}{2}\int \epsilon_o^T D X z dA dz$$

The last two integrals represent coupling between middle-surface deformations and bending or twisting which vanish if the laminate is symmetric with respect to the middle surface, but must be retained in this development.

In integrating through the thickness, it is assumed that each layer is a different homogeneous orthotropic material, but none of the matrices depends on z. For example, the last integral in the aforementioned energy expression consequently becomes

$$\frac{1}{4}\sum_{i=1}^{n}(h_{i+1}^2 - h_i^2)\int_{A_i} \epsilon_o^T D X dA$$

where h_i is the z coordinate of the bottom of layer i and n is the number of layers.

The element matrix is obtained by differentiation of the energy integral with respect to the nodal displacements, as is usually done

$$K_{ij} = \frac{\partial^2 U}{\partial u_i \partial u_j}$$

where u_i, u_j represent all of the nodal displacements and rotations.

To proceed with development of the element, it is necessary to define the matrices that relate strains in the element to nodal displacements. These expressions are taken from the paper by Utku (1973), and the details of the derivation will not be repeated here. The nodal displacements in the x direction at the three nodal points are represented by

$$\bar{u} = \begin{bmatrix} u_1 \\ u_2 \\ u_3 \end{bmatrix}$$

and the same convention is used to represent the other components of nodal displacement.

The displacements in the interior of the element u, v, θ_x, θ_y, and w^* are each interpolated from their nodal values by the same linear function. For example,

$$u = \frac{1}{2A}[x\ y\ 1]\begin{bmatrix} y_2 - y_3 & y_3 - y_1 & y_1 - y_2 \\ x_3 - x_2 & x_1 - x_3 & x_2 - x_1 \\ x_2 y_3 - x_3 y_2 & x_3 y_1 - x_1 y_3 & x_1 y_2 - x_2 y_1 \end{bmatrix}[\bar{u}]$$

To get the interpolation for deflection in the y direction, u is replaced by v and $\bar{u}$ by $\bar{v}$, and so forth. In this expression, A represents area of the element, and x_1 and y_1 are the coordinates of node 1, and so forth.

It follows that the strains on the middle surface ϵ_o are given by

$$\epsilon_o = \frac{1}{2A}[M\ N]\begin{bmatrix} \bar{u} \\ \bar{v} \end{bmatrix}$$

and the curvatures X are given by

$$X = \frac{1}{2A}[N\ -M]\begin{bmatrix} \bar{\theta}_x \\ \bar{\theta}_y \end{bmatrix}$$

where

$$N = \begin{bmatrix} 0 & 0 & 0 \\ x_3 - x_2 & x_1 - x_3 & x_2 - x_1 \\ y_2 - y_3 & y_3 - y_1 & y_1 - y_2 \end{bmatrix}$$

and

$$M = \begin{bmatrix} y_2 - y_3 & y_3 - y_1 & y_1 - y_2 \\ 0 & 0 & 0 \\ x_3 - x_2 & x_1 - x_3 & x_2 - x_1 \end{bmatrix}$$

Development of the expression for out-of-plane shear strain γ in terms of nodal displacements is the principal contribution of Utku's (1973) paper. It is given by

$$\gamma = \begin{bmatrix} \gamma_{xz} \\ \gamma_{yz} \end{bmatrix} = \frac{1}{4A}\left(\begin{bmatrix} y_2 - y_3 & y_3 - y_1 & y_1 - y_2 \\ x_3 - x_2 & x_1 - x_3 & x_2 - x_1 \end{bmatrix} \begin{bmatrix} 1 & 0 & 0 & -y_1 & 0 & 0 & x_1 & 0 & 0 \\ 0 & 1 & 0 & 0 & -y_2 & 0 & 0 & x_2 & 0 \\ 0 & 0 & 1 & 0 & 0 & -y_3 & 0 & 0 & x_3 \end{bmatrix} \right.$$

$$\left. + \begin{bmatrix} y_2 - y_3 & y_3 - y_1 & y_1 - y_2 & 0 & 0 & 0 & \frac{2A}{3} & \frac{2A}{3} & \frac{2A}{3} \\ x_3 - x_2 & x_1 - x_3 & x_2 - x_1 & -\frac{2A}{3} & -\frac{2A}{3} & -\frac{2A}{3} & 0 & 0 & 0 \end{bmatrix} \right) \begin{bmatrix} \bar{w} \\ \bar{\theta}_x \\ \bar{\theta}_y \end{bmatrix}$$

or

$$\gamma = \frac{1}{4A}[H] \begin{bmatrix} \bar{w} \\ \bar{\theta}_x \\ \bar{\theta}_y \end{bmatrix}$$

Perhaps it should be noted that some terms are missing from the matrices which are the end result in Utku (1973).

In the computer implementation of this element, the matrices relating strains to nodal displacements are calculated from the aforementioned algebraic expressions. The remaining problems are calculated numerically, layer by layer. Since the strain-displacement matrices contain only constants, integration over the area is trivial. Each of the five energy integrals is processed to yield the corresponding submatrix of the element, stiffness matrix, and the results are added into the proper location in the element stiffness matrix. The program then goes on to process the next layer which may have different material properties. The first term of the energy integral, for example, represents the membrane deformation part of the strain energy U_m.

$$U_m = \frac{1}{2}\int \epsilon_o^T D \epsilon_o dA dz$$

Integrating through the thickness, this becomes

$$U_m = \frac{1}{2}\sum_{i=1}^{n}(h_{i+1} - h_i)\int_{A_i} \epsilon_o^T D \epsilon_o dA$$

where h_i is the z coordinate of the bottom of layer i and n is the number of layers.

Substituting for strains in terms of nodal displacements and taking second partial derivatives of the energy with respect to nodal displacements, results in the submatrix k_m, which represents the membrane part of the element stiffness matrix.

$$k_m = \frac{\partial^2 U_m}{\partial u_i \partial u_j} = \frac{1}{4A}\sum_{i=1}^{n}(h_{i+1} - h_i)[M\ N]^T D_i [M\ N]$$

Using the same process

$$k_b = \frac{1}{12A}\sum_{i=1}^{n}(h_{i+1}^3 - h_i^3)[N\ -M]^T D_i [N - M]$$

$$k_s = \frac{1}{16A}\sum_{i=1}^{n}(h_{i+1} - h_i)[H]^T D_i' [H]$$

$$k_{A1} = \frac{1}{8A}\sum_{i=1}^{n}(h_{i+1}^2 - h_i^2)[M\ N]^T D[N\ -M]$$

$$k_{A2} = \frac{1}{8A}\sum_{i=1}^{n}(h_{i+1}^2 - h_i^2)[N\ -M]^T D_i[M\ N]$$

Rotations $\bar{\theta}_x$ and $\bar{\theta}_y$ are row degrees of freedom for k_{A1}. Displacements $\bar{u}$ amd $\bar{v}$ are row degrees of freedom for k_{A2}. The element stiffness matrix K is

$$K = k_m + k_b + k_s + k_{A1} + k_{A2}$$

One term in each of the aforementioned summations, which represents stiffness contribution of the current layer, is computed. Each stiffness coefficient from each submatrix is added into the appropriate location in the element stiffness matrix. The program then goes on to the next layer until all layers have been processed. The element stiffness matrix is then complete.

ELEMENT PERFORMANCE

The three-node shell element developed herein should prove convenient for modeling irregular shapes with cutouts, as well as for analysis of unsymmetric sandwich composite laminates and includes out-of-plane shear deformation. In comparison with other elements, it may be termed LU71 (Laminated-Utku-1971). Calculations show that the LU71 gives accurate solutions for both thick and thin plates, converges uniformly for various shapes, and appears robust. Convergence with mesh refinement is slower than that of the two elements used for comparison, but neither of those elements can fill the need for which the LU71 was developed.

Figure 2 shows one of the test problems used to verify the element, which illustrates the coupling of bending and in-plane deflection. Table 1 shows calculated deflections for four cases, all with the same loading. These results are exact and can be easily calculated by hand because strains are constant throughout. The first case is a four-layer symmetric laminate with fibers only in the 0° and 90° directions. The second case represents modeling where 0° and 90° elements are overlayed. Results are identical. The third case is an unsymmetric laminate. Loads applied at the middle surface cause bending and out-of-plane deflection. The fourth case is identical to the third, except that the laminate thickness is 0.1 in. instead of the 1.0 in. used in the first three cases. Deflection at the center of stiffness is the same in all four cases. The increase in the value of the deformation in the X direction UX for the third and fourth cases is due to rotation and the calculation of the UX at the middle surface.

In this example, Material I was used as defined by Reddy (1980) with $E_1 = 10.6 \times 10^6$ psi.

$$E_1/E_2 = 25$$
$$G_{12}/E_2 = 0.5$$
$$G_{23}/E_2 = 0.2$$
$$\nu_{12} = 0.25$$

Figure 3 provides a convergence comparison of the LU71 element with the DKT element (Batoz and others, 1980), which is type 53 in ANSYS (DeSalvo and Swanson, 1985), and with Reddy's eight-node isoparametric element (Reddy, 1980) for a thin simply supported plate. All converge to the same result. The DKT type B solution has element diagonals at −45° rather than +45°, and convergence is slower, but still very good.

The convergence in figure 4 is compared with that in figure 3 for a moderately thick plate. The DKT element is much too stiff because it has no shearing deflections. The LU71 element converges to the same result as that of Reddy's (1980) isoparametric element.

In figures 3 and 4, Reddy's result is plotted as being equivalent to 32 triangular shell elements, since it is estimated that 32 triangular shell elements represent about the same computational effort as the four isoparametric quadrilateral elements actually used. Reddy uses 2 by 2 integration in his examples, but for some 8-node elements, this can result in an ill-conditioned or even singular matrix in structures with no or few support constaints. In application to airframes, it is believed that 3 by 3 integration would be required. With a 3 by 3 integration, the result will be a little less accurate than that shown in the figures.

The DKT element (Batoz and others, 1980) gives outstanding performance in most bending problems. Its convergence rate is, however, sensitive to boundary conditions and element shape. For membrane deformations, it is a constant stress triangle, as in the LU71. Lack of shearing deformations is its greatest weakness in analysis of composites.

Utku (1973) gives seven examples comparing the performance of the shell element formulation used here with an earlier formulation for isotropic homogeneous plates. The examples show uniform convergence regardless of element shape. The formulation used here converges faster than the earlier one for equilateral triangular elements; but the convergence is slower when the element has an obtuse angle.

Table 2 shows some results for thin plates obtained by using the LU71. The example is a 48-in.^{2} homogeneous isotropic plate with $E = 10.6 \times 10^6$ psi, $\nu = 1/3$ and a concentrated load of 16 lb at the center. All edges were fixed. One quarter of the plate was modeled by 242 elements in a regular mesh. Elements were right triangles with the short side 2.18 in. long. Since the LU71 includes shear deformation, it should give larger deflections for the thicker plates but the same deflection for very thin plates. Table 2 shows that the LU71 gives results as expected at the plate side length/thickness ratio a/h of 500. At $a/h = 1000$, the LU71 has a small error; for thinner plates, the errors become greater.

CONCLUDING REMARKS

The three-node shell element proves to be convenient for modeling irregular shapes with cutouts, and is also suitable for analysis of unsymmetric sandwich composite laminates. It appears to be robust and gives accurate results for both thick and thin shells.

Formulation of the element is straightforward. It is believed that this formulation can be used as a basis for a dynamic element that may provide much improved numerical efficiency.

Ames Research Center
Dryden Flight Research Facility
National Aeronautics and Space Administration
Edwards, California, March 1, 1988

APPENDIX—COMPARISON OF EXPERIMENTAL DEFLECTIONS OF GRAPHITE COMPOSITE PLATES WITH FINITE ELEMENT CALCULATIONS

Introduction

Three graphite-composite plates were built and tested to verify the performance of the LU71 finite element. The LU71 element was developed during 1986 and implemented for testing in a program called LCSHEL during 1987. It is a three-node C° element for analysis of plates and shells made of composite materials with an arbitrary symmetric or unsymmetric stacking sequence. The LU71 was developed to meet an immediate need in the STARS program (Gupta, 1984) for analysis of airframes made of unsymmetric laminated composites and also to provide a foundation for future development of a finite dynamic element with greatly improved numerical efficiency. The experimental work described here was intended to verify the treatment and manipulation of material properties for symmetric and unsymmetric laminates and the overall correctness of analysis by using the element.

Plate Fabrication

Three graphite fiber composite plates were fabricated. The graphite fiber was supplied in a 12-in.-wide roll of unidirectional fiber with a few cross-strands of glass fiber to maintain shape and fiber spacing. The specified weight of this material was 0.033 lb/ft^2, and specified tensile strength of the fiber was 450,000 psi. The resin used was Hexcell 2410 with 2184 hardener. Plates were placed on a flat surface, vacuum bagged, and cured at room temperature.

Plate A was a four-layer unidirectional plate 9.25 by 12.0 in. with an average thickness of 0.0303 in. The fiber fraction was 0.572 by weight. Calculated volume fractions were $v_f = 0.474$ fiber, $v_m = 0.458$ resin, and 0.068 voids. This plate was cut into strips for tension tests in the fiber and transverse directions for determination of material properties.

Plate B was a six-layer unsymmetric (0/0/0/90/90/90) plate 12.0 by 12.0 in. with an average thickness of 0.04311 in. The fiber fraction was 0.582 by weight. Calculated volume fractions were $v_f = 0.494$ fiber, $v_m = 0.480$ resin, and 0.0259 voids. Thickness was measured at 1-in. grid points on a surface plate with a 1/10,000-in. dial indicator. The average thickness was 0.04311 in. with a standard deviation of 0.0058 in. This plate was trimmed to 11.3 by 11.3 in. for use in a five-point bend test.

Plate C was an eight-layer symmetric (0/0/90/90/90/90/0/0) plate, 12.0 by 12.0 in. with an average thickness of 0.0549 in. The fiber fraction was 0.637 by weight. Calculated volume fractions were $v_f = 0.517$ fiber, $v_m = 0.399$ resin, and 0.084 voids. Thickness was measured at 1-in. grid points on a surface plate with a 1/10,000-in. dial indicator. The average thickness was 0.0549 in. with a standard deviation of 0.0046 in. This plate was trimmed to 11.3 by 11.3 in. for use in a five-point test.

Material Properties

Material properties were determined from tests on specimens cut from plate A. Specimens were approximately 1 in. wide by 9 in. long. Metal plates 2.5 in. long were glued to the ends of the specimens (to avoid crushing), leaving a 4-in. test length. Biaxial electric resistance strain gages were glued to both sides of the specimens and all gages were read individually.

Material properties in the fiber direction were consistent. Unfortunately, the test machine for measuring transverse properties failed to work properly, and some data were lost. Since there was some uncertainty in the correct value of the transverse modulus, the material properties in table 3 show a high estimate for E_2 (upper bound) and a low estimate for E_2 (lower bound).

Finite-element calculations were performed for both sets of properties so that the effect of this uncertainty could be assessed. Adjustments in properties to account for differences in fiber volume fractions were done using relations from Chamis (1984) and Jones (1975).

The in-plane shear modulus G_{12} was determined from a four-point bend test, supported at three corners and loaded at the fourth corner. The shear modulus is determined directly as given by Chandra (1976). When limited to the linear range and neglecting self-weight, this simplifies to

$$G_{12} = \frac{3a^2}{h^2}\frac{P}{w}$$

in which a is plate side length, h is plate thickness, P is load, and w is deflection at the point of loading. The value of G_{12} is larger than would be expected from Chamis (1984), but numerical experiments show that this has a negligible influence on results. This larger value of in-plane shear modulus could be associated with slight waviness in the fibers.

Figure 5 shows the subscripting convention and notation for elastic constants.

Plate Bending Tests

Plates B and C were tested in five-point bending with supports at each of the four corners and a concentrated load at the center (fig. 6). Supports were set 0.35 in. from the corners of the plates so that the distance between supports was 10.6 in. Loading was by deadweights, and deflections were measured by a microscope with a resolution of 1/10,000 in.

Plots of load versus deflection data are shown for the six-layer unsymmetric plate in figure 7 and for the eight-layer symmetric plate in figure 8. Lines through the data points were fitted by least squares. The plots show good linearity for both loading and unloading.

Comparisons to Calculations

The finite-element grid used for calculations is shown in figure 9. Calculations were done with the LU71 element in the LCSHEL program. Additional calculations, not included here, were done with ANSYS, and agreement between the two programs was good.

Experimental and calculated results are compared in table 4. Since there was some uncertainty about the values of E_2, calculations were done separately using the high estimate (upper bound) for E_2 and the low estimate (lower bound) for E_2.

Results for the six-layer unsymmetric plate (plate B) show excellent agreement. Using the upper-bound properties, the calculated result is 2.3 percent stiffer than the experimental result; using the lower-bound properties, the calculated result is 2.2 percent softer than the experimental result.

Agreement between results from experiment and calculations for the eight-layer symmetric plate is not optimum, but still adequate. Using the upper-bound properties results in a calculation 5.7 percent stiffer than the experiment, while using the lower-bound properties results in a calculation that is 2.2 percent stiffer than the experiment. The average deviation between calculations and experiment is 3.9 percent.

Conclusion

Comparison of results from plate bending experiments and finite-element calculations show very good agreement, and support the conclusion that the finite-element program is using composite material properties correctly.

It is believed that the resulting discrepancies are due primarily to imperfections in technique for fabricating the composite plates and performing basic property measurements.

REFERENCES

Batoz, Jean-Louis, Klaus-Jurgen Bathe, and Lee-Wing Ho, "A Study of Three-Node Triangular Plate Bending Elements," *International Journal for Numerical Methods in Engineering*, vol. 15, 1980, pp. 1771–1812.

Chandra, Ramesh, "On Twisting of Orthotropic Plates in a Large Deflection Regime," *AIAA Journal*, vol. 14, no. 8, Aug. 1976, pp. 1130–1131.

Chamis, C.C., "Simplified Composite Micromechanics Equations for Hygral, Thermal, and Mechanical Properties," *SAMPE Quarterly*, Apr. 1984, pp. 14–18.

DeSalvo, G.J., and J.A. Swanson, *ANSYS Engineering Analysis System User's Manual*, Swanson Analysis Systems, Inc., Houston, Pennsylvania, 1985.

Gallagher, R.H., "Shell Elements," *Proceedings of the World Congress on Finite Methods in Structural Mechanics*, vol. 1, Bournemouth, Dorset, England, 1975.

Gallagher, R.H., "Geometrically Nonlinear Shell Analysis," *Proceedings of the International Conference on Finite Elements in Nonlinear Solid and Structural Mechanics*, Col-1/Col-26, Geilo, Norway, 1978.

Gupta, K.K., "Finite Dynamic Element Formulation for a Plane Triangular Element," *International Journal for Numerical Methods in Engineering*, vol. 14, 1979, pp. 1431–1448.

Gupta, K.K., *STARS — A General-Purpose Finite Element Computer Program for Analysis of Engineering Structures*, NASA RP-1129, 1984.

Jones, Robert M., *Mechanics of Composite Materials*, Scripta Book Co. (McGraw-Hill), 1975.

Martin, H.C., *Stiffness Matrix for a Triangular Sandwich Element in Bending*, TR32-1158, Jet Propulsion Laboratory, Pasadena, California, 1967.

Melosh, R.J., *A Flat Triangular Shell Element Stiffness Matrix*, AFFDL-TR-66-80, Air Force Flight Dynamics Laboratory, Wright-Patterson Air Force Base, Ohio, 1966.

Reddy, J.N., "A Penalty Plate-Bending Element for the Analysis of Laminated Anisotropic Composite Plates," *International Journal for Numerical Methods in Engineering*, vol. 15, 1980, pp. 1187–1206.

Utku, Senol, "On Derivation of Stiffness Matrices With C° Rotation Fields for Plates and Shells," AFFDL-TR-71-160, Air Force Third Conference on Matrix Methods in Structural Mechanics, Wright-Patterson Air Force Base, Ohio, 1973.

Weisshaar, T.A., "Aeroelastic Tailoring — Creative Uses of Unusual Materials," AIAA 87-0976-CP, AIAA/ASME/ASCE/AHS 28th Structures, Structural Dynamics, and Materials Conference, Apr. 1987.

TABLE 1. DEFLECTIONS FOR IN-PLANE LOADING

Stack sequence	UX, 10^{-4} in.	UY, 10^{-6} in.	UZ, 10^{-2} in.	θ_y, 10^{-3} rad
0/90/90/0	−0.36207	0.69629	0	0
Superimposed 0 and 90	−0.36207	0.69629	0	0
0/90/90/0	−1.0038	1.9303	0.13898	−0.27797
0/0/90/90	−10.038	19.303	13.898	−27.797

TABLE 2. CENTER DEFLECTION OF THIN SQUARE PLATES WITH FIXED EDGES[a]

h, in.	a/h	b/h	Thin plate theory, in.	LU71, in.	Difference, percent
0.96	50	2.27	$0.2180(10^{-3})$	0.2329×10^{-3}	+6.8
0.48	100	4.55	$0.1744(10^{-2})$	0.1840×10^{-2}	+5.5
0.096	500	22.7	0.2180	0.2231	+2.3
0.048	1000	45.5	1.744	1.684	−3.4
0.032	1500	68.2	5.887	5.287	−10.0
0.024	2000	90.9	13.95	11.56	−17.2

[a]Plate side length = a = 48 in.
Thickness = h
Length of short element side = b = 2.18 in.

TABLE 3. MATERIAL PROPERTIES

	Low E_2 estimate	High E_2 estimate
Fiber modulus, E_f, 10^6 psi	30.13	30.09
Resin modulus, E_m, 10^6 psi	0.2138	0.2484
ν_m	0.3000	0.3000
ν_f	0.1383	0.0811
Plate B, six layers		
E_1, 10^6 psi	15.38	15.38
E_2, 10^6 psi	0.8463	0.9784
ν_{12}	0.2181	0.1886
ν_{21}	0.0120	0.0120
G_{12}, 10^6 psi	1.849	1.849
Plate C, eight layers		
E_1, 10^6 psi	15.64	15.65
E_2, 10^6 psi	0.7231	0.8365
ν_{12}	0.1911	0.1868
ν_{21}	0.0088	0.0100
G_{12}, 10^6 psi	1.938	1.938

TABLE 4. COMPARISON OF EXPERIMENTAL MEASUREMENT AND FINITE-ELEMENT CALCULATIONS OF STIFFNESS (LOAD/DEFLECTION RATIO) OF GRAPHITE COMPOSITE PLATES

Plate	Properties	Finite-element calculated stiffness, lb/in.	Experimental stiffness, lb/in.	Difference, percent
Plate B				
(Six-layer)	High E_2 estimate	6.504	6.359	+2.3
	Low E_2 estimate	6.223	6.359	−2.2
	Average	6.364	6.359	0.0
Plate C				
(Eight-layer)	High E_2 estimate	14.45	13.67	+5.7
	Low E_2 estimate	13.97	13.67	+2.2
	Average	14.21	13.67	+3.9

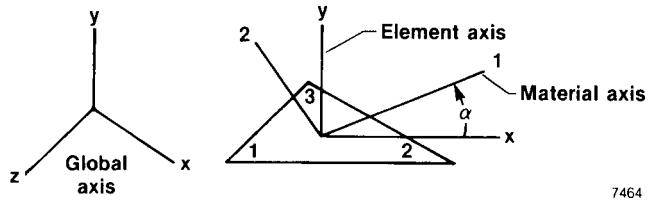

Figure 1. Coordinate systems.

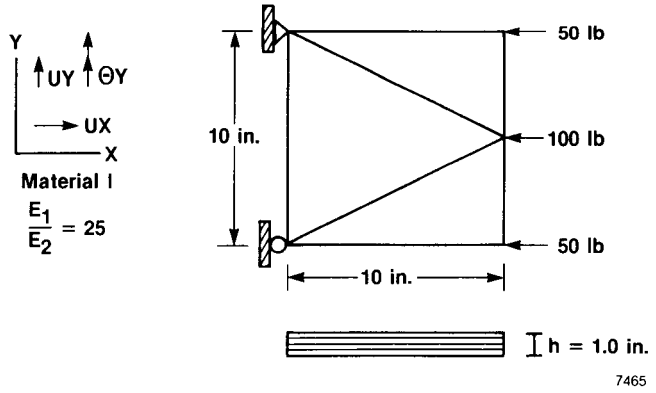

Figure 2. In-plane loading example.

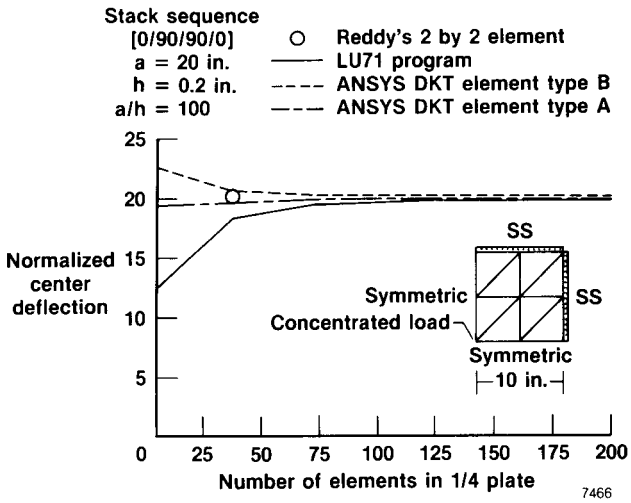

Figure 3. Comparison of convergence for thin plate.

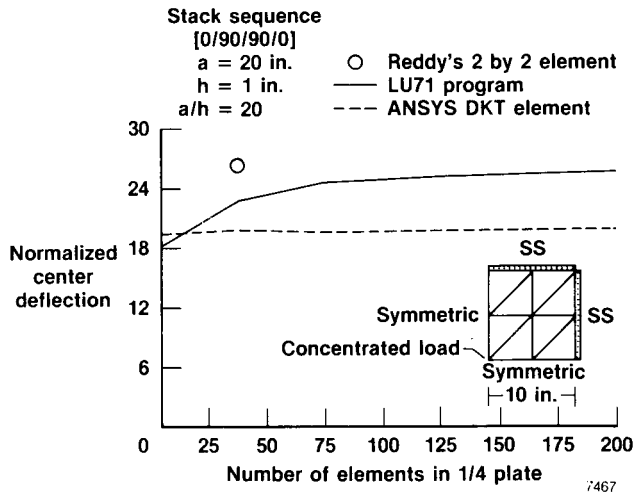

Figure 4. Comparison of convergence for thick plate.

The strains for plane stress due to load in direction 1 are

$$ {}^{1}\varepsilon_1 = \frac{\sigma_1}{E_1}, \quad {}^{1}\varepsilon_2 = \left(-\frac{V_{12}}{E_1}\right)\sigma_1 $$

where the loading direction is denoted by left superscript.

Similarly, the strains due to load in direction 2 are

$$ {}^{2}\varepsilon_1 = \left(-\frac{V_{21}}{E_2}\right)\sigma_2, \quad {}^{2}\varepsilon_2 = \frac{\sigma_2}{E_2} $$

therefore, the stiffness matrix for the stress-strain relations for plane stress in orthotropic material in terms of the engineering constants are

$$ Q_{11} = \frac{E_1}{1 - V_{12}V_{21}} $$

$$ Q_{12} = \frac{V_{12}E_2}{1 - V_{12}V_{21}} = \frac{V_{21}E_1}{1 - V_{12}V_{21}} $$

$$ Q_{22} = \frac{E_2}{1 - V_{12}V_{21}}, \quad Q_{66} = G_{12} $$

$$ \begin{bmatrix} \sigma_1 \\ \sigma_2 \\ \tau_{12} \end{bmatrix} = \begin{bmatrix} Q_{11} & Q_{12} & 0 \\ Q_{12} & Q_{22} & 0 \\ 0 & 0 & Q_{66} \end{bmatrix} \begin{bmatrix} \varepsilon_1 \\ \varepsilon_2 \\ \gamma_{12} \end{bmatrix} $$

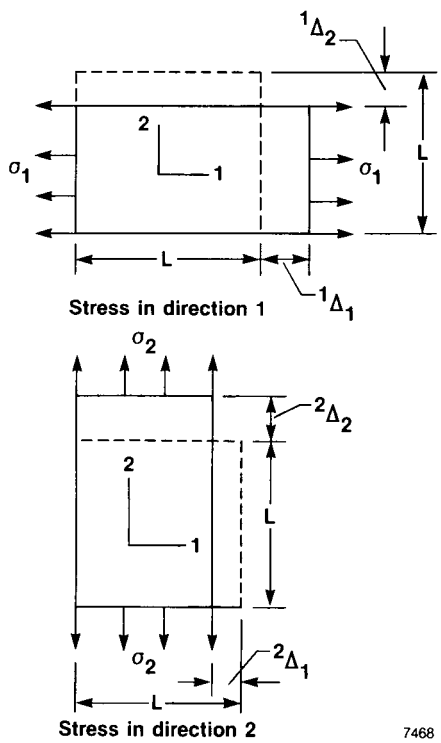

Figure 5. Material property definitions (Jones, 1975, pp. 39–46).

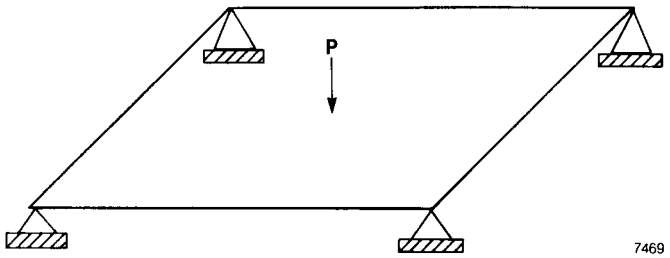

Figure 6. Five-point bending test.

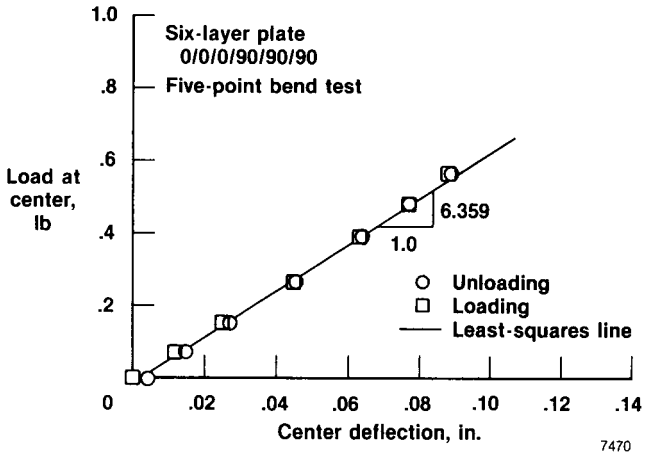

Figure 7. Bending test of six-layer unsymmetric plate.

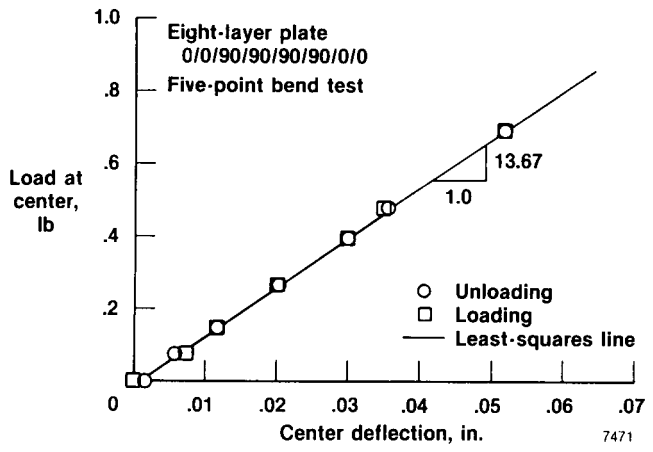

Figure 8. Bending test of eight-layer symmetric plate.

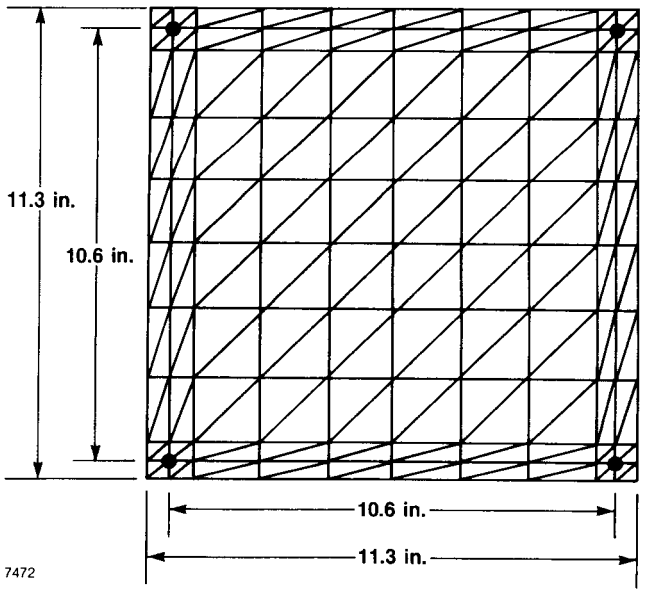

Figure 9. Finite-element mesh used for calculation of stiffness of graphite composite plates.

NASA National Aeronautics and Space Administration

Report Documentation Page

1. Report No.	2. Government Accession No.	3. Recipient's Catalog No.
NASA TM-4125		

4. Title and Subtitle

A Three-Node C° Element for Analysis of Laminated Composite Sandwich Shells

5. Report Date
June 1989

6. Performing Organization Code

7. Author(s)

C. Wayne Martin, S.F. Lung, and K.K. Gupta

8. Performing Organization Report No.
H-1479

10. Work Unit No.
RTOP 533-02-51

9. Performing Organization Name and Address

NASA Ames Research Center
Dryden Flight Research Facility
P.O. Box 273, Edwards, CA 93523-5000

11. Contract or Grant No.

13. Type of Report and Period Covered
Technical Memorandum

12. Sponsoring Agency Name and Address

National Aeronautics and Space Administration
Washington, DC 20546

14. Sponsoring Agency Code

15. Supplementary Notes

Point of contact: Dr. C. Wayne Martin, Prof. of Engineering Mechanics, University of Nebraska, 212 Bancraft Hall, Lincoln, NE 68588-0347

16. Abstract

A three-node flat shell element with C° rotation fields has been developed for analysis of arbitrary composite shells. The element may consist of any number of orthotropic layers, each layer having different material properties and angular orientation. The formulation includes coupling between bending and extension, which is essential for analysis of unsymmetric laminates. Shearing deflections are included, since laminated and sandwich construction frequently results in shear stiffness much smaller than bending stiffness. Formulation of the element is straightforward, and calculation of its stiffness matrix is simple and fast. Convergence of solutions with mesh refinement is uniform for both thin and thick shells and is insensitive to element shape, although not as rapid as some other elements that lack one or more capabilities of the newly developed element. An experimental verification of the shell element is reported in the appendix.

17. Key Words (Suggested by Author(s))	18. Distribution Statement
Composite shell elements Finite elements Structural analysis	Unclassified — Unlimited Subject category 39

19. Security Classif. (of this report)	20. Security Classif. (of this page)	21. No. of pages	22. Price
Unclassified	Unclassified	16	A02

NASA FORM 1626 OCT 86

For sale by the National Technical Information Service, Springfield, VA 22161-2171.

NASA-Langley, 1989